



# The Effect of Sliding Speed on Film Thickness and Pressure Supporting Ability of a Point Contact Under Zero Entrainment Velocity Conditions

Peter M. Thompson  
Case Western Reserve University, Cleveland, Ohio

William R. Jones, Jr.  
Glenn Research Center, Cleveland, Ohio

Mark J. Jansen  
AYT Corporation, Brook Park, Ohio

Joseph M. Prahl  
Case Western Reserve University, Cleveland, Ohio

## The NASA STI Program Office . . . in Profile

Since its founding, NASA has been dedicated to the advancement of aeronautics and space science. The NASA Scientific and Technical Information (STI) Program Office plays a key part in helping NASA maintain this important role.

The NASA STI Program Office is operated by Langley Research Center, the Lead Center for NASA's scientific and technical information. The NASA STI Program Office provides access to the NASA STI Database, the largest collection of aeronautical and space science STI in the world. The Program Office is also NASA's institutional mechanism for disseminating the results of its research and development activities. These results are published by NASA in the NASA STI Report Series, which includes the following report types:

- **TECHNICAL PUBLICATION.** Reports of completed research or a major significant phase of research that present the results of NASA programs and include extensive data or theoretical analysis. Includes compilations of significant scientific and technical data and information deemed to be of continuing reference value. NASA's counterpart of peer-reviewed formal professional papers but has less stringent limitations on manuscript length and extent of graphic presentations.
- **TECHNICAL MEMORANDUM.** Scientific and technical findings that are preliminary or of specialized interest, e.g., quick release reports, working papers, and bibliographies that contain minimal annotation. Does not contain extensive analysis.
- **CONTRACTOR REPORT.** Scientific and technical findings by NASA-sponsored contractors and grantees.

- **CONFERENCE PUBLICATION.** Collected papers from scientific and technical conferences, symposia, seminars, or other meetings sponsored or cosponsored by NASA.
- **SPECIAL PUBLICATION.** Scientific, technical, or historical information from NASA programs, projects, and missions, often concerned with subjects having substantial public interest.
- **TECHNICAL TRANSLATION.** English-language translations of foreign scientific and technical material pertinent to NASA's mission.

Specialized services that complement the STI Program Office's diverse offerings include creating custom thesauri, building customized data bases, organizing and publishing research results . . . even providing videos.

For more information about the NASA STI Program Office, see the following:

- Access the NASA STI Program Home Page at <http://www.sti.nasa.gov>
- E-mail your question via the Internet to [help@sti.nasa.gov](mailto:help@sti.nasa.gov)
- Fax your question to the NASA Access Help Desk at 301-621-0134
- Telephone the NASA Access Help Desk at 301-621-0390
- Write to:  
NASA Access Help Desk  
NASA Center for AeroSpace Information  
7121 Standard Drive  
Hanover, MD 21076



# The Effect of Sliding Speed on Film Thickness and Pressure Supporting Ability of a Point Contact Under Zero Entrainment Velocity Conditions

Peter M. Thompson  
Case Western Reserve University, Cleveland, Ohio

William R. Jones, Jr.  
Glenn Research Center, Cleveland, Ohio

Mark J. Jansen  
AYT Corporation, Brook Park, Ohio

Joseph M. Prah  
Case Western Reserve University, Cleveland, Ohio

Prepared for the  
Annual Meeting  
sponsored by the Society of Tribologists and Lubrication Engineers  
Orlando, Florida, May 20–24, 2001

National Aeronautics and  
Space Administration

Glenn Research Center

This report contains preliminary findings, subject to revision as analysis proceeds.

Trade names or manufacturers' names are used in this report for identification only. This usage does not constitute an official endorsement, either expressed or implied, by the National Aeronautics and Space Administration.

Available from

NASA Center for Aerospace Information  
7121 Standard Drive  
Hanover, MD 21076  
Price Code: A03

National Technical Information Service  
5285 Port Royal Road  
Springfield, VA 22100  
Price Code: A03

Available electronically at <http://gltrs.grc.nasa.gov/GLTRS>

# The Effect of Sliding Speed on Film Thickness and Pressure Supporting Ability of a Point Contact Under Zero Entrainment Velocity Conditions

Peter M. Thompson  
Case Western Reserve University  
Cleveland, Ohio 44106

William R. Jones, Jr.  
Glenn Research Center  
Cleveland, Ohio 44135

Mark J. Jansen  
AYT Corporation  
Cleveland, Ohio 44142

Joseph M. Prah  
Case Western Reserve University  
Cleveland, Ohio 44106

## ABSTRACT

A unique tribometer is used to study film forming and pressure supporting abilities of point contacts at zero entrainment velocity (ZEV). Film thickness is determined using a capacitance technique, verified through comparisons of experimental results and theoretical elastohydrodynamic lubrication (EHL) predictions for rolling contacts. Experiments are conducted using through hardened AISI 52100 steel balls, Polyalphaolefin (PAO) 182 and Pentaerythritol Tetraheptanoate (PT) lubricants, and sliding speeds between 2.0-12.0 m/s. PAO-182 and PT are found to support pressures up to 1.1 GPa and 0.67 GPa respectively. Protective lubricant films ranging in thickness between 90-210 nm for PAO-182 and 220-340 nm for PT are formed. Lubricants experience shear stresses between 14-22 MPa for PAO-182 and 7-16 MPa for PT at shear rates of  $10^7 \text{ sec}^{-1}$ . The lubricant's pressure supporting ability most likely results from the combination of immobile films and its transition to a glassy solid at high pressures.

## INTRODUCTION

Ball bearings that employ liquid lubricants are found in many spacecraft applications, including momentum and reaction wheels used in attitude control systems (ACS). Retainer instability can be linked to many performance and reliability issues and can result in erratic increases in driving torque and large vibrations caused by retainer instability.

These instabilities can be continuous or sudden and cause retainer fracture, resulting in bearing failure.

One way to prevent these retainer-related problems is to eliminate the retainer all together. However, theoretical predictions of no pressure supporting ability and no film thickness between adjacent, counter rotating balls, producing zero entrainment velocity, have produced skepticism about retainerless ball bearing operation.

Recently, retainerless bearing work performed by Kingsbury (1978, 79, 80, 82, 83, 90, 92), Hunter (1987), Olson (1990), Schritz (1994), DeLucie (1992), and Jones (1997, 1996) indicated evidence of a protective film between point contacts at ZEV. In all these tests, there was never a ball-ball failure, but rather all failures occurred between ball-race contacts.

In order to study ZEV; the ball-ball contact must be isolated from all other factors. Shogrin (1998) developed a tribometer to isolate this type of contact and performed several tests at ZEV. In this work, Shogrin (1998) demonstrated zero entrainment films of polyalphaolefin were capable of supporting contact stresses up to 0.57 GPa at sliding speeds ranging between 6.0 and 10.0 m/s. It also showed ZEV sustainable films up to 28.8 minutes with film thickness ranging between 0.10 and 0.14  $\mu\text{m}$ . The current work extends experimentation with this tribometer to other lubricants and a broader range of sliding speeds and contact stresses.

## EXPERIMENTAL

### ENTRAINMENT VELOCITY

Entrainment velocity is defined as the velocity of the lubricant between two balls at the point of contact. Within a retainerless bearing, the balls are rotating in the same direction with equal rotational velocity. Therefore, at the point contact, the surface velocities are of equal magnitude and opposite in direction. This is defined as zero entrainment velocity (ZEV).

Sliding speed is determined by subtracting the two surface velocities at the point contact. For example, a 10 m/s sliding speed indicates the surface velocity of each ball is 5 m/s in opposite directions.

### TRIBOMETER

The tribometer, shown in Figure 1, was designed (Shogrin 1998) to study ball-to-ball contact in detail. This tribometer can simulate a wide variety of entrainment conditions, including surface velocities from 0.1 to 10 m/s, Hertzian contact stresses to 4 GPa, pure rolling, rolling with any degree of slip, and steady and unsteady velocity profiles. It is also possible to conduct experiments on sustained ZEV, zero entrainment reversal, and impact loading. In doing so, measurements of contact load, temperature, and velocity are recorded along with capacitance, resistance, dissipation, spindle separation distance, spindle torque, and oil bath

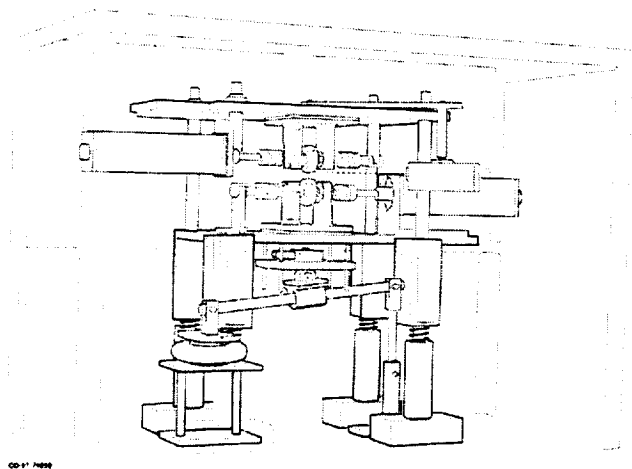


Figure 1 - Overview of Tribometer

temperature.

Contact film thickness is determined using two methods. The first is a capacitance measurement, discussed in detail in Shogrin's thesis (1998). Capacitance is calculated using an HP LCR meter. The second method employs two Linear Variable Differential Transducers (LVDTs) positioned collinearly with the point of contact and are used to determine an approach velocity and approximate ball separation.

An infrared pyrometer, with an accuracy of  $\pm 1^\circ\text{C}$ , is used to measure the meniscus temperature, while a thermocouple records the temperature of the oil reservoir. Mercury slip rings are implemented to transmit and receive electrical signals from the rotating spindles. The entire apparatus is placed on an air table to reduce vibration and it is encased in a plexiglas housing continuously purged with nitrogen to prevent lubricant oxidation.

Two grade 100, through hardened ( $R_c = 62$ ), AISI 52100, steel balls are used. The balls are 64 cm in diameter with a surface roughness ( $R_a$ ) of  $0.02\text{ }\mu\text{m}$  and an out of roundness of  $2.5\text{ }\mu\text{m}$ . Each had a surface finish, surface metallurgy, and curvature imitating balls typically used in high precision bearings.

A specialized beryllium-copper, non-contact rotating torque sensor is mounted inline with the motor and the upper spindle unit. The only possible location to mount the torque sensor inline with the motors was outside of the locating bearings of the test specimen on the upper spindle unit. Therefore, the torque measured is a combination of the friction in the bearings and the shearing in the lubricant at the contact between the two test specimens. The solution to this issue is described in the procedures section.

### LUBRICANT

The first set of tests was conducted with NYE 182, a filtered polyalphaolefin (PAO). The lubricant contains two additives: tricresyl phosphate at 1.0 weight percent, used to reduce wear, and a hindered phenol at 0.5 weight percent, added to reduce oxidation of the oil. PAOs are often used in aerospace bearings, gyro bearings, and precision rotating equipment. Their usefulness is attributed to their low temperature fluidity, low volatility, and oxidative stability to over  $100^\circ\text{C}$ . Similar PAOs with various molecular weights have been used in the

other retainerless bearing studies (Kingsbury 1992, Olson 1990, DeLucie 1992, Woodwell et al 1994).

Pentaerythritol Tetraheptanoate (PT) is an organic ester based lubricant. It has excellent thermal stability and usefulness over a wide range of temperature to 204°C. As a group, these types of advanced esters exhibit excellent low-temperature viscosity properties, high viscosity indices, and good lubricity in addition to their thermal stability. The Air Force employs these lubricants in high-speed jet turbines used in supersonic aircraft. PT is a pure compound and therefore has no additives (Gunderson et al 1962).

The lubricant is supplied to the contact in two ways. The lower ball is partially submerged in an oil bath and the lubricant is injected onto the upper ball, just above the point of ball-ball contact. The injector supplied lubricant to the upper ball at a rate of  $\approx 1$  ml/sec. To prevent over-heating, which could cause lubricant degradation, and to slow heating in longer tests, the lubricant is passed through a cooling bath before being injected onto the top ball.

## PROCEDURE

### SPECIMEN PREPARATION

After the test specimen was press fit onto the shaft assembly, the surface of each ball was ultrasonically cleaned in hexane, acetone, and finally methanol for a period no less than twenty minutes each. An IR analysis of each specimen was done to assure that any residual oils had been removed from the surface. An optical microscope was used to examine the ball surfaces before testing. The surfaces were visually inspected and photographed to identify any pre-test surface cracks or flaws, which may influence the results. Once the inspection was completed, the shaft assemblies were installed into the tribometer. To assure the ball cleanliness, the ball surfaces were wiped down with a lint-free cloth containing each of the three solvents. The test specimens were dried in an enclosed nitrogen environment. Finally, the balls were coated with the test lubricant. Once all the tests were completed with NYE 182, the balls were replaced. Once the testing began, with the prescribed lubricant, the specimens were not subsequently cleaned. All tests with one lubricant were run with the same specimens.

## SETUP

A LabVIEW™ program regulates the data collection and motion control of the experiment. At the onset of each test the capacitance meter is calibrated. After confirming the accuracy of the capacitance meter, the test is started. The lubricator is used to assure a constant fully flooded condition at the contact point. The final approach velocity for these tests is 0.15  $\mu\text{m}/\text{sec}$ . Once the specimens come into contact, the load is then increased to the desired value. Finally, the test is completed when the tribometer is shutdown manually or automatically if one of the limit criteria is surpassed. The data is saved and analyzed.

## LIMITS

The specimens used in this experiment are expensive, difficult to manufacture, and complicated to replace. For these reasons, specialized shutdown criteria were utilized to insure the safety of the ball surfaces. Film thickness, monitored by the capacitance, and lubricant temperature are the limit criteria.

### ROLLING EHL TESTS

In order to confirm the accuracy of the capacitance method to calculate film thickness, pure rolling tests were performed. Calculated film thickness approximations were within the theoretical central and minimum film thickness, verifying the approximation. Details are fully described in Thompson's thesis (2000).

### ZERO ENTRAINMENT TESTS

Once the capacitance to film thickness approximations were verified for each lubricant and specimen set, zero entrainment velocity (ZEV) tests were conducted. The test's set up was identical to the set up for the rolling tests.

The goal of the ZEV tests was to determine the maximum load the counter rotating contact could support at a given sliding speed before the film thickness reached an unsafe dimension, i.e. the dielectric break down thickness. As stated previously, the capacitance limit is the best representation of the film thickness at the contact and was therefore used as the primary limit imposed on the health of the lubricant film.

Once the surfaces came into contact, the load was increased at a rate of 0.45 N/sec until the tribometer automatically shutdown as a result of the limit criteria being exceeded.

## TORQUE MEASUREMENTS

The position of the torque sensor in-line with the upper spindle unit is such that the torque measured is that of the shearing of the lubricant in the contact between the two specimens and the torque created by the friction in the bearings that locate the upper spindle.

In order to isolate the torque increases caused by only the shearing during counter rotation, two sets of tests were conducted. The first set of tests was at zero entrainment velocity. The pressures at the contact were slowly increased until the predefined limits shutdown the experiment. The second set of tests was performed in pure rolling, where the spindle velocities and loads exactly mimicked that of the zero entrainment velocity tests. This was done to insure that at any given load and speed condition, the torque caused by the bearing friction was the same for both the ZEV and the pure rolling tests. The torque measured in the pure rolling tests was subtracted from the torque measured in the ZEV tests, leaving only the torque caused by the shearing of the lubricant during the ZEV tests. Three trials at each condition were performed and results averaged.

## SURFACE WEAR

Many precautions to prevent surface contact and wear were taken to ensure the safety of the specimens. However, there is inevitably some amount of surface damage as a result of asperity contact through the lubricating film. In order to quantify the surface damage incurred during zero entrainment tests, the lower specimen was removed from the tribometer half way through the set of tests and then again after all of the ZEV tests were completed. The specimen surfaces were visually inspected with an optical microscope. Pictures of the specimen's surface were taken at different locations around the ball. This was done for both sets of specimens. The results of this inspection, along with the discovered surface damage, are discussed at the end of the next section.

## RESULTS

### ROLLING EHL TESTS

The results gathered show that the film thickness calculated by the capacitance method lies between the central and minimum film thickness determined from the Hamrock and Dowson (1981) equations. The capacitance model used in this study does not differentiate between the minimum and central film thickness for the contact zone and thus it is reasonable to assume that the calculated film thickness will lie somewhere between the two. This indicates a good correlation between the two film thickness approximations and therefore verifies the accuracy of the capacitance method.

A common parameter used to estimate the degree of surface contact is the lambda ratio ( $\Lambda$ ). The  $\Lambda$ -ratio is calculated by dividing the minimum film thickness by the composite surface roughness ( $\sigma_c$ ), which is the square root of the sum of the squares of the ball and race surface roughnesses ( $R_{RMS}$ ). In general,  $\Lambda$  ratios greater than three indicate complete surface separation. A transition from full EHL to mixed lubrication (partial EHL film and some asperity contact) occurs in the  $\Lambda$  range between 1 and 3. At  $\Lambda$ -values less than one, boundary lubrication ensues with continual asperity contact and little contribution from fluid films.

$\Lambda$ -values were calculated for a variety of sliding speeds. At an entrainment velocity of 2.0 m/s, the  $\Lambda$ -value has an average of approximately 4. When the entrainment velocity is increased to 2.5 m/s, the  $\Lambda$ -value increases to 4.7. Finally, at entrainment velocity of 1.5 m/s the  $\Lambda$ -value is 2.8. The values indicate an EHL type lubricating film.

### ZERO ENTRAINMENT VELOCITY TESTS

The zero entrainment velocity tests were designed to determine the maximum pressure supporting ability of a lubricating film under ZEV conditions. The load at which the thickness of the supporting film reached the dielectric breakdown thickness was designated the maximum load that the film could support, i.e. the film began to act like a short circuit.

### PRESSURE SUPPORTING ABILITY AT ZEV

The maximum pressure that a lubricant film could support under ZEV conditions was determined for sliding speeds ranging between 2.0 and 10.0 m/s for the PAO, and between 5.0 and 12.0 m/s for



Pentaerythritol Tetraheptanoate. Four trials were performed at each speed. The results indicate a strong relationship between the sliding speed and the film's load capacity. As the sliding speed was decreased, the pressure that the film was able to support decreased. Table 1 lists the maximum pressure the lubricant film could support at each

Table 1 – Maximum Hertzian Stress (GPa) supported by test lubricants at ZEV conditions

Sliding Speed	PAO-182	Pentaerythritol Tetraheptanoate
2.0	0.58±0.02 / (84±3)	N/A
3.0	0.71±0.01 / (103±2)	N/A
4.0	0.81±0.02 / (117±3)	N/A
5.0	N/A	0.38±0.01 / (55±2)
6.0	0.88±0.03 / (128±4)	0.45±0.04 / (65±6)
8.0	1.06±0.06 / (154±9)	0.54±0.01 / (78±2)
10.0	1.11±0.03 / (161±4)	0.61±0.02 / (89±3)
12.0	N/A	0.67±0.04 / (97±6)

sliding speed.

No pressure supporting ability was found below a sliding speed of 2.0 m/s for PAO 182 and 5.0 m/s for PT. The balls simply contacted each other without forming a protective lubricating film.

#### FILM THICKNESS

When the film thickness was compared over the range of loads and sliding speeds, it was observed that the film thickness is dependent upon the sliding speed at the contact. As the sliding speed was increased, the thickness of the lubricant film also increased. Over the duration of the test, as the load is increased, the film thickness decreased until the limit criteria was exceeded.

#### TORQUE MEASUREMENTS

With the PAO-182, approximately equal torques for all the sliding speeds tested at Hertzian Stresses between 0.525 GPa and 0.645 GPa were observed. Torque started at 0.02 Nm at low stress and went to 0.05 Nm at higher stress. At stresses above 0.645 GPa the torque data begins to diverge. At this point, the torque for the slowest sliding speed has the highest value (0.0636 Nm at 2.0 m/s), while the torque for the fastest sliding speed has the lowest value (0.0441 Nm at 8.0 m/s). This divergence trend continues as the loads are increased. As reported early in this text, the higher the sliding speed the higher the load was at failure.

Torque trends for the PT were similar, except the divergence at higher speeds was not observed. Torque was 0.005 Nm at 0.28 GPa and linearly reached 0.35 Nm at 0.75 GPa.

#### SHEAR STRESS AND SHEAR RATE

In a counter rotating system such as this, the shear stresses and strain rates in the lubricant are exceedingly high. The shear stress in this experiment can be calculated directly from the torque measurements.

For the PAO-182, it was observed that the shear stress generally stays between 15 and 20 MPa throughout the range of contact stresses. For sliding speeds ranging between 2 and 6 m/s, the shear stress gradually increases as the load increases, indicating that the torque is increasing at a faster rate than the Hertzian Contact Area. The 8.0 m/s data shows very high shear stresses at low loads. This is a result of the very small contact zone that increases the shear stress. The same phenomenon was observed with PT at the high speeds (12 m/s) and low Hertzian Stresses (0.3 GPa, 43.5 ksi). For the PT, the sliding speeds ranging between 5.0 and 10.0 m/s produce shear stresses on the order of 10 to 15 MPa (1.4 to 2.2 ksi).

Because of the counter rotation of the balls, the lubricant also sees very large shear rates in addition to the high shear stresses.

For both the PAO-182 and PT, the shear rate starts at some base value that is relatively constant across all of the sliding speeds, approximately  $2.3 \times 10^7 \text{ sec}^{-1}$  for PAO-182 and  $1.0 \times 10^6 \text{ sec}^{-1}$  for PT. The shear rates increase as the film thickness decreases over the duration of the test. The shear rates for the maximum speed tested for both lubricants reach values as high as  $4.5 \times 10^7 \text{ sec}^{-1}$  at a sliding speed of 8.0 m/s for PAO-182, and  $3.5 \times 10^7 \text{ sec}^{-1}$  at 12.0 m/s for PT. The implications of these high shear stresses and shear rates will be discussed in the next section.

#### ENERGY DISSIPATION

As the lubricant is brought around into the contact, a certain amount of energy, resulting from the shearing in the contact, must be dissipated into each ball. The energy that is dissipated into the ball is equal to the work done on the fluid through the Hertzian contact area. From the work, the temperature of the fluid film can be calculated. A detailed description appears in Thompson (2000).

The contact temperatures rise at a constant rate for all of the sliding speeds and the slope of the curve for the contact temperature is similar to the slope of the meniscus temperature curve.

## VISCOSITY

An attempt to better understand the physics of the contact was made by determining the relationship between the torque measured and the viscosity of the lubricant expected under the high temperatures and pressures in the contact. The absolute viscosity of a fluid is a function of the pressure and temperature of the fluid. In 1966, Roelands et al introduced a relationship for viscosity as a function of temperature and pressure. The calculations are described in detail by Thompson (2000).

Once the pressure and the temperature dependence on viscosity had been established, the film temperatures calculated in the previous section were inserted into the viscosity relationship. Once the viscosities were known, they were used to calculate a torque. The theoretical torque calculated using the above equation for viscosity should be equal to the torque measured by the sensor. For PAO-182, the measured values for the torque are greater than the torque calculated using the pressure-temperature viscosity function. This trend exists everywhere except for sliding speeds of 2.0 and 3.0 m/s at the low stresses, < 0.6 GPa.

For PT, a significant difference between the measured torque and the torque calculated from the theoretical viscosity was observed. In some cases, the measured torque is as much as one to two orders of magnitude larger than the calculated torque.

## SURFACE WEAR

With a small  $\Lambda$ -value such as the ones associated with ZEV contacts ( $\Lambda \approx 1.5$ ), some surface damage is expected. This is exactly what is found upon closer examination of the surfaces. After the first set of ZEV tests were conducted to determine maximum pressure supporting ability, the lower spindle unit was removed from the tribometer. The ball surface was wiped down with a lint-free wipe containing hexane to dissolve any excess lubricant still on the ball. The ball was then inspected using an optical microscope and surface damage was assessed.

The subsequent inspection of the lower spindle/ball assembly revealed scratches aligned with the sliding

direction inside the Hertzian contact radius. It is believed the scratches were caused by asperities on the ball or by particles in the oil that extended through the film and scratched the balls. These scratches also were observed by Shogrin (1998).

Eight cracks perpendicular to the sliding direction and extending beyond the Hertzian contact region, as shown in Figure 2, were also discovered on the ball. These cracks extended an average of 1.2 mm on either side of the contact region. The lower ball had been viewed under the microscope before and after running twenty-five ZEV tests and such cracks had not been observed (Shogrin 1998). After forty-five additional tests the cracks were discovered. Thirty-five extra tests were performed after the discovery of the cracks and confirmed repeatability of all the tests. After all tests were completed with PAO-182, the upper spindle unit was also removed and the upper ball was viewed under the optical microscope. Cracks running perpendicular to the direction of motion were also discovered.

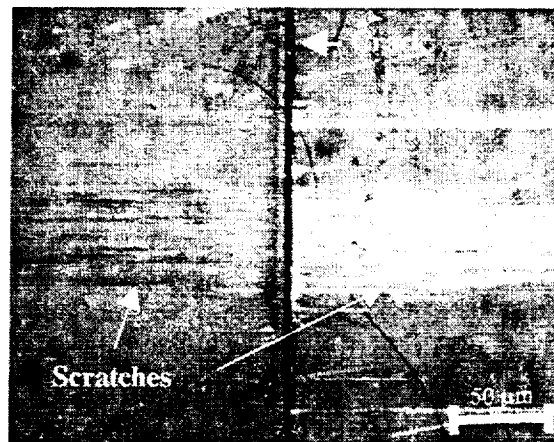


Figure 2 - Surface Crack

## DISCUSSION

### SHEAR RATE DEPENDENT VISCOSITY

The measured torque should be equal to the torque calculated from the pressure-temperature dependent viscosity relationship. However, when the measured torque was compared to the calculated torque, a discrepancy was found. This discrepancy is the result of the effects of shear rate on the viscosity. Under very high shear rates, such as in this experiment, the viscosity increases. In some cases,

the shear rate plays a more significant role than either temperature or pressure. Below are two models for viscosity as a function of shear rate (Tichy 1998).

Power Law:

$$\eta = m\dot{\gamma}^{n-1}$$

Eyring model:

$$\eta = \frac{\tau_0}{\dot{\gamma}} \arcsin(\lambda_0 \dot{\gamma})$$

Both of the above equations are well known functions for the viscosity under high shear rate conditions. However, both equations involve lubricant specific constants,  $m$  and  $n$  for the power law, and  $\tau_0$  and  $\lambda_0$  for the Eyring model. At the present time no research has been done in this area for the lubricants tested in this study. In order to accurately obtain these constants for the PAO-182 and PT, additional independent experiments using a much simpler geometry need to be conducted. It is likely that once the shear rate is taken into account in the viscosity model, the measured torque will equal the calculated torque, thereby providing a better understanding of the actual viscosity of the lubricant in the contact.

## BOUNDARY LAYER PHENOMENA

There are a variety of possible reasons for pressure supporting ability at ZEV. The first possibility to be discussed is boundary layer phenomena. The present EHL theories are unable to model these films. Research (Smeeth et al 1996) dealing with ultra-thin lubrication indicates the presence of immobile films in EHL contacts at low rolling speeds. The TCP additive in PAO-182 may have also produced a reactive layer.

The PAO-182 used in this study was formulated with tricresyl phosphate (TCP), and plausible that it played a roll in film formation. It is believed that TCP forms a surface film consisting of a reactive iron phosphate ( $\text{FePO}_4$ ) layer and an adsorbed phosphate derivative layer (Woodwell et al 1994). Layers are typically formed at elevated temperatures, especially around asperities (Ashby et al 1991). The ZEV conditions would provide the elevated temperatures needed to form a TCP film. However, it is unlikely that the surface protection provided by the TCP film could solely account for the

pressure supporting ability at ZEV. Also, it would not explain the pressure supporting ability of the PT, a pure compound. Additionally, DeLucie and Olson's experiments were successful using un-formulated oils, suggesting a more complex mechanism of surface protection.

## THICK IMMOBILE LAYERS

Another possible reason for the pressure supporting ability could result from immobile films. Immobile layers have been demonstrated by Fuks (1960). In this experiment, two disks were submerged in various mineral oils remaining separated by a thin layer of oil, even after several hours under load.

Other static squeeze tests demonstrating the presence of immobile layers were performed by Georges et al (1993) and supported by others (Israelachvili 1998). The films, said not to participate in hydrodynamic flow, were detected on several substrates with a variety of oils. However, these tests were not performed with high loads or relative motion.

Using ultra-thin film interferometry to study immobile films in EHL contacts, Smeeth et al (1996) discovered immobile surface films as thick as 20 nm at a Hertzian Stress of 0.52 GPa and a rolling speed of 0.1 m/s. The immobile surface film has a viscosity much greater than the bulk lubricant. This indicates that the contact operates within a viscous boundary layer. The immobile, EHL film that is formed is much thicker than the film predicted from the viscosity of the bulk lubricant. These temperature independent films had thickness that did not vary with entrainment velocity and disappeared when the rotation was stopped (Cann and Spikes 1994).

Cann and Spikes (1994) concluded that the rolling motion trapped the lubricant in the contact before the viscous action could cause it to flow out. When the rolling stopped, the lubricant was able to flow out of the contact. When Cann and Spikes (1994) reduced the rolling speed to between 0.01 and 0.001 m/s, there was sufficient time for the viscous effects to cause the lubricant to flow out of the contact before it could be trapped, causing the surfaces to contact. The results also indicated there is a speed/stress relationship. When the sliding speed between the surfaces decreases, the pressure it can support also decreases. The work done in this study echoes Spikes' finding.

## GLASSY SOLID

Another plausible scenario for the pressure supporting of a ZEV is that under very high loads and shear stresses the lubricant undergoes a transition to a glassy solid that by itself can support a load. Oils used for lubrication, such as those in this study, contain linear and highly branched hydrocarbons. These lubricants can undergo two types of transition. The first is a glass transition connected to the non-crystallized component of the oil and the second is a phase transition associated with the wax in the oil (Alsaad et al 1978). The transition to glass is based on the glass transition temperature,  $T_g$ . If the operating temperature of the lubricant is less than the glass transition temperature, the lubricant will behave as a glassy solid (Alsaad et al 1978). The viscosity of this glassy solid is of the order of  $10^7$  Pa·s at the time of transition from a liquid to a solid phase (Yasutomi et al. 1984). For most lubricants at atmospheric pressure, the glass transition temperature is well below 0°C. However, as the pressure in the lubricant increases, so does the glass transition temperature. The glass transition temperature increases with pressure at a rate of 80-350°C/GPa (Alsaad et al 1978). Therefore, it is plausible that under the high contact stresses seen in this study, the lubricant is operating as a glassy solid at the temperature experienced during the tests. Since the lubricant is acting as a solid within the counter rotating contact, it is likely to shear or cleave as it undergoes the very high shear stress (10-30 MPa) at some mid-plane in the contact zone. This would result in a solid-like, protective coating on the surface of each ball that together would form a pressure supporting film.

This cleaving condition in a normal bearing is described as the limiting shear stress of the lubricant. Smith first proposed the limiting shear stress in a lubricant in 1959 when he was unable to explain that traction in an EHL contact hardly ever exceeded one tenth of the pressure using a Newtonian viscous flow model with a pressure dependent viscosity. The limiting shear stress of lubricant oil is the material property determining the maximum shear stress that can be transmitted in an EHD contact (Bair and Winer 1979), and thus once the limiting shear stress is surpassed, i.e. the lubricant is a glassy solid, the lubricant will cleave. At high shear rates the lubricant will behave like a glassy solid. Studies (Bair and Winer 1979) have also shown the limiting shear stress is independent of the rate of shear in the contact, but instead is only dependent upon the pressure and temperature. If

these lubricants do display a glassy characteristic within the contact zone, it is possible that this solid like behavior is the reason for a pressure supporting ability at a ZEV contact.

The temperature-pressure dependency could also be used to explain the maximum pressure supporting abilities found during these experiments. During the tests, as the pressure was increased, the temperature also increased due to shearing friction. It is possible that the test failed because the contact temperature surpassed the glass transition temperature, causing a phase change back into a liquid, resulting in contact failure. This conclusion is supported by Alsaad et al (1978), who found that glassy states did not exist at high sliding speeds unless the lubricant was under a very high load.

## CONCLUSION

A specially designed tribometer was used to investigate the pressure supporting and film-forming ability of two commonly used lubricating oils, PAO-182 and PT, in zero entrainment velocity flow. Despite contradictory theoretical predictions, a pressure supporting film was formed at ZEV. In the case of PAO-182, films capable of supporting pressures as high as 1.1 GPa at sliding speeds of 10.0 m/s were formed and maintained. PT supported pressures as high as 0.67 GPa at a sliding speed of 12.0 m/s. These films ranged in thickness between 90 and 210 nm for PAO-182 and 220 and 340 nm for PT.

The experiments also showed the lubricants experienced shear stresses ranging between 14 and 22 MPa for PAO-182 and between 7 and 16 MPa for PT. The lubricants also underwent shear rates on the order of  $10^7$  sec<sup>-1</sup>, all while maintaining a pressure supporting film.

The pressure supporting ability of these films is most likely results from the combination of the lubricant's transition to a glassy solid at the very high pressures found in the contact, and immobile films formed on the surface of the test specimens.

Additional work in this field needs to be conducted to determine the constants in the viscosity shear rate model. Once the viscosities of the lubricant are accurately quantified, there will be a better understanding of the state of the lubricant. A second set of experiments should also be conducted to determine the glass transition temperatures at

different pressures. This knowledge will ultimately contribute to an understanding of the pressure supporting ability of a zero entrainment velocity point contact.

## REFERENCES

- Alsaad, M., Bair, S., Sanborn, D. M., and Winer, W. O., "Glass Transition in Lubricants: Its Relation to Elastohydrodynamic Lubrication (EHD)", *Trans. of ASME*, **100**, July 1978, 404-417.
- Ashby, M.F., Abulawi, J., Kong, H.S., "Temperature Maps for Frictional Heating in Dry Sliding", *Tribol. Trans.*, **34**, 4, 1991, 577-587.
- Bair, S., and Winer, W. O. "Shear Strength Measurements of Lubricants at High Pressure," *Journal of Lubrication Technology*, **101**, July 1979, pp. 251-256
- Cann, P.M., Spikes, H.A., "The Behavior of Polymer Solutions in Concentrated Contacts: Immobile Surface Layer Formation", *Trib. Trans.*, **37**, 3, 1994, 580-586.
- DeLucie, D., "Load Carrying Capacity of Counter Rotating Balls in a Retainerless Bearing", Masters of Science Thesis, Massachusetts Institute of Technology, (1992).
- Fuks, G.I., "The Properties of Solutions of Organic Solids in Liquid Hydrocarbons at Solid Surfaces", in B.V. Deryagin (ed.), *Research in Surface Forces*, **1**, (1960).
- Georges, J.M., Millot, S., Loubet, J.L., Tonck, A., "Drainage of Thin Liquid Films Between Relatively Smooth Surfaces", *J. Chem. Phys.*, **98**, May 1993, 9.
- Gunderson, Reigh C., Hart, Andrew W., *Synthetic Lubricants*, Reinhold Publishing Corporation, New York, 1962, 388-400
- Hamrock, B.J. Dowson, D., "Isothermal Elastohydrodynamic Lubrication of Point Contacts, Part III, Fully Flooded Results", *Journal of Lubrication Technology*, **99**, April 1977, 264-276.
- Hamrock, B.J., Dowson, D., *Ball Bearing Lubrication. The Elastohydrodynamics of Elliptical Contacts*, John Wiley & Sons, Inc., (1981).
- Israelachvili, J.N., "Measurements and Relation Between the Dynamic and Static Interactions Between Surfaces Separated by Thin Liquid and Polymer Films", *Pure and Applied Chemistry*, **60**, 1998, 1473-1478.
- Jones, W.R., Jr., Shogrin, B.A., Kingsbury, E.P., "Long Term Performance of a Retainerless Bearing Cartridge With and Oozing Flow Lubricator for Spacecraft Applications", 4<sup>th</sup> International Rolling Element Bearing Symposium, Orlando, Florida, April 1997, NASA-TM 107492, Aug. (1997).
- Jones, W.R., Jr., Toddy, T.J., Predmore, R., Shogrin, B.A., Herrera-Fierro, P., "The Effect of ODC-Free Cleaning Techniques on Bearing Lifetimes in the Parched Elastohydrodynamic Regime", 2<sup>nd</sup> Aerospace Environmental Technology Conference, Huntsville, Alabama, Aug 1996, NASA-TM 107322, (Sept. 1996).
- Kingsbury, E.P., "Ball-Ball Load Carrying Capacity in Retainerless Angular-Contact Bearings", *J. Lube. Tech.*, **104**, (1982), 327-329.
- Kingsbury, E.P., "Ball Contact Locus in an Angular Contact Bearing", *J. Lubr. Tech.*, **105**, 2, (1983), 166-170.
- Kingsbury, E.P. "Ball Motion Perturbation in an Angular Contact Ball Bearing", *ASLE Trans.*, **25**, 3, (1982), 279-282.
- Kingsbury, E.P., "Basic Speed Ratio of an Angular Contact Bearing", *J. Lube. Tech.*, **102**, (July 1980), 391-394.
- Kingsbury, E.P., "Dynamic and Coupling Influences on Basic Speed Ratio of an Angular Contact Bearing", *Wear*, **63**, (1980), 189-196.
- Kingsbury, E.P., "Influences on Polymer Formation Rate in Instrument Ball Bearings", *Tribol. Trans.*, **35**, 1, (1992), 184-188.
- Kingsbury, E.P., "Large Bearing Operation Without Retainer", *Lube. Eng.*, **35**, 9, (1979), 517-520.
- Kingsbury, E.P., "Lubricant-Breakdown in Instrument Ball Bearings", *J. Lube. Tech.*, **100**, (July 1978), 386-394.
- Kingsbury, E.P., Schritz, B., Prael, J., "Parched Elastohydrodynamic Lubrication Film Thickness Measurements in an Instrument Ball Bearing", *Trib. Trans.*, **33**, 1, (1990), 11-14.
- Kingsbury, E.P., "Slip Measurement in an Angular Contact Ball Bearing", *J. Lube. Tech.*, **105**, (April 1983), 162-165.
- Kingsbury, E.P., "Torque Variations in Instrument Ball Bearings", *ASLE Trans.*, **8**, (1965), 435-441.
- Kingsbury, E.P., Walker, R., "Motion of an Unstable Retainer in an Instrument Ball Bearing", *J. Trib.*, **116**, (Apr. 1994), 202-208.
- Olsen, A.J., "Load Carrying Capacity Between Lubricated Counter Rotating Balls", Masters of Science Thesis, Massachusetts Institute of Technology, (1990).
- Roelands, C. J. A., "Correlation Aspect of the Viscosity-Temperature-Pressure Relationship of Lubricating Oils" Druk, V.R.B., Groningen, Netherlands, 1966.
- Schritz, B., Jones, W.R., Jr., Prael, J.P., Jansen, R.H., "Parched Elastohydrodynamic Lubrication: Instrumentation and Procedure", *Trib. Trans.*, **37**, 1, (1994), 13-22.
- Shogrin, B. A., "Experimental Determination of Load Carrying Capacity of Point Contacts at Zero Entrainment Velocity", Ph. D. Dissertation, Case Western Reserve Univ., Cleveland, OH, (1998).

Smeeth, M., Spikes, H. A. and Gansel, S. "The Formation of Viscous Surface Films by Polymer Solutions: Boundary or Elastohydrodynamic Lubrication." *Trib. Trans.*, **39**, 3, 1996, 720-725.

Smeeth, M. Spikes, H.A., "Central and Minimum Elastohydrodynamic Film Thickness at High Contact Pressure," ASME Preprint 96-TRIB-22, 1996.

Smith F. W. "Lubricant Behavior in a Concentrated Contact System--The Castor Oil-Steel System", *Wear*, **2**, No. 4, 1959, pp. 250-263.

Thompson, P. M., "Effects of Sliding Speed on the Film Thickness and Pressure Supporting Ability of a Point Contact Under Zero Entrainment Velocity Conditions" Masters Thesis, Case Western Reserve Univ., Cleveland, OH, (2000)

Tichy, John A, "Rheological Modeling of Thin Film Lubrication", *Tribology Issues and Opportunities in MEMS*, Netherlands, 1998, pp. 175-183.

Woodwell, R.G., Miller, L. Anderson, C., "Alkaline Cleaning: Its Effects on Tricresyl Phosphate Coated Bearing Steels", *Proc. Of Non-Ozone Depleting Chemical Cleaning and Lubrication of Space System Mech. Components for Multi-Year Operations*, Denver, CO., (Sept. 1994).

Yasutomi, S., Bair, S., and Winer, W. O. " An Application of a Free Volume Model to Lubrication Rheology," *ASME Journal of Tribology*, **106**, No. 2, 1984



REPORT DOCUMENTATION PAGE			Form Approved OMB No. 0704-0188	
Public reporting burden for this collection of information is estimated to average 1 hour per response, including the time for reviewing instructions, searching existing data sources, gathering and maintaining the data needed, and completing and reviewing the collection of information. Send comments regarding this burden estimate or any other aspect of this collection of information, including suggestions for reducing this burden, to Washington Headquarters Services, Directorate for Information Operations and Reports, 1215 Jefferson Davis Highway, Suite 1204, Arlington, VA 22202-4302, and to the Office of Management and Budget, Paperwork Reduction Project (0704-0188), Washington, DC 20503.				
1. AGENCY USE ONLY (Leave blank)		2. REPORT DATE December 2000		3. REPORT TYPE AND DATES COVERED Technical Memorandum
4. TITLE AND SUBTITLE  The Effect of Sliding Speed on Film Thickness and Pressure Supporting Ability of a Point Contact Under Zero Entrainment Velocity Conditions			5. FUNDING NUMBERS  WU-274-00-00-00	
6. AUTHOR(S)  Peter M. Thompson, William R. Jones, Jr., Mark J. Jansen, and Joseph M. Pahl				
7. PERFORMING ORGANIZATION NAME(S) AND ADDRESS(ES)  National Aeronautics and Space Administration John H. Glenn Research Center at Lewis Field Cleveland, Ohio 44135-3191			8. PERFORMING ORGANIZATION REPORT NUMBER  E-12531	
9. SPONSORING/MONITORING AGENCY NAME(S) AND ADDRESS(ES)  National Aeronautics and Space Administration Washington, DC 20546-0001			10. SPONSORING/MONITORING AGENCY REPORT NUMBER  NASA TM-2000-210566	
11. SUPPLEMENTARY NOTES Prepared for the Annual Meeting sponsored by the Society of Tribologists and Lubrication Engineers, Orlando, Florida, May 20-24, 2001. P.M. Thompson and J.M. Pahl, Department of Mechanical and Aerospace Engineering, The Case School of Engineering, Case Western Reserve University, 10900 Euclid Avenue, Cleveland, Ohio 44106; W.R. Jones, Jr., NASA Glenn Research Center; M.J. Jansen, AYT Corporation, 2001 Aerospace Parkway, Brook Park, Ohio 44142. Responsible person, W.R. Jones, Jr., organization code 5140, 216-433-6051.				
12a. DISTRIBUTION/AVAILABILITY STATEMENT  Unclassified - Unlimited Subject Category: 27  Available electronically at <a href="http://gltrs.grc.nasa.gov/GLTRS">http://gltrs.grc.nasa.gov/GLTRS</a> This publication is available from the NASA Center for AeroSpace Information, 301-621-0390.			12b. DISTRIBUTION CODE	
13. ABSTRACT (Maximum 200 words)  A unique tribometer is used to study film forming and pressure supporting abilities of point contacts at zero entrainment velocity (ZEV). Film thickness is determined using a capacitance technique, verified through comparisons of experimental results and theoretical elastohydrodynamic lubrication (EHL) predictions for rolling contacts. Experiments are conducted using through hardened AISI 52100 steel balls, Polyalphaolefin (PAO) 182 and Pentaerythritol Tetraheptanoate (PT) lubricants, and sliding speeds between 2.0 to 12.0 m/s. PAO 182 and PT are found to support pressures up to 1.1 GPa and 0.67 GPa respectively. Protective lubricant films ranging in thickness between 90 to 210 nm for PAO 182 and 220 to 340 nm for PT are formed. Lubricants experience shear stresses between 14 to 22 MPa for PAO 182 and 7 to 16 MPa for PT at shear rates of $10^7 \text{ sec}^{-1}$ . The lubricant's pressure supporting ability most likely results from the combination of immobile films and its transition to a glassy solid at high pressures.				
14. SUBJECT TERMS  Tribology; Elastohydrodynamics			15. NUMBER OF PAGES 16	
			16. PRICE CODE A03	
17. SECURITY CLASSIFICATION OF REPORT  Unclassified	18. SECURITY CLASSIFICATION OF THIS PAGE  Unclassified	19. SECURITY CLASSIFICATION OF ABSTRACT  Unclassified	20. LIMITATION OF ABSTRACT	